

Role of heavy meson exchange in near threshold $NN \rightarrow d\pi$

C. J. Horowitz

Nuclear Theory Center and Department of Physics, Indiana University, Bloomington, Indiana 47405

(Received 21 July 1993)

The total cross section for $NN \rightarrow d\pi$ very near threshold is calculated in a simple distorted wave impulse approximation including one-body, pion rescattering, and sigma and omega meson exchange current (MEC) contributions. Calculations with MEC are in good agreement with recent TRIUMF measurements while calculations without MEC are significantly smaller. Thus the MEC mechanism, which was proposed to explain a large enhancement in the $pp \rightarrow pp\pi^0$ cross section, is consistent with $NN \rightarrow d\pi$ data.

PACS number(s): 13.75.Cs, 21.30.+y

I. INTRODUCTION

Recent measurements of the (near threshold) pion production cross section in $pp \rightarrow pp\pi^0$ were much larger than expected [1]. This result can be explained by a σ meson exchange current (MEC) which enhances both the axial charge and s -wave pion production [2,3]. This could have important implications for our understanding of pion production and absorption reactions and axial MEC.

An important further test of this proposed MEC mechanism is provided by the bound state production reaction $pn \rightarrow d\pi^0$. Here the near threshold cross section is accurately known from a recent TRIUMF measurement [4]. This reaction samples different spin and isospin matrix elements of the MEC than $pp \rightarrow pp\pi^0$. Furthermore, there is now an important contribution from the d state of the deuteron. Therefore, this cross section provides a check on the MEC operator used to explain $pp \rightarrow pp\pi^0$.

In this paper we calculate $pn \rightarrow d\pi^0$ using the same MEC model as Ref. [2]. The formalism is presented in Sec. II while Sec. III lists results for a variety of potential models. We conclude in Sec. IV that this MEC mechanism is consistent with the $pn \rightarrow d\pi^0$ data.

II. DISTORTED WAVE IMPULSE APPROXIMATION FORMALISM

Very near threshold, the angular momentum barrier favors the production of s -wave pions. In this paper, we calculate only s -wave pion production. This requires the initial nucleons to be in a 3P_1 state. As in Ref. [2] our distorted wave impulse approximation (DWIA) formalism includes contributions from the diagrams in Figs. 1(a)–1(c). Figure 1(a) is the one-body contribution where the s -wave pion-nucleon coupling is related to the axial charge of a single nucleon. Figure 1(b) describes the pion rescattering contribution where a pion is emitted from one nucleon and scatters off of the second nucleon. Finally Fig. 1(c) describes the heavy meson MEC contributions. Here the exchange of a σ or ω meson modifies the nucleon's axial charge. This leads to a two-body contribution to the axial current.

We evaluate these three diagrams in a simple one-boson-exchange model that is consistent with the one-

boson-exchange potential used to generate the initial and final wave functions. We consider a number of different potential models in Sec. III.

The one-body contribution is very straightforward to evaluate. It can be generated from an interaction Hamiltonian which describes the coupling of a nucleon to an s -wave pion [5]

$$H_{\text{int}} = \frac{f}{m_\pi} q_0 \gamma_5 \gamma_0 \left(\frac{1}{2} q_0 \right)^{1/2} \tau_0. \quad (1)$$

Here q_0 is the energy of the pion. Near threshold this reduces to,

$$H_{\text{int}} \approx f \left(\frac{m_\pi}{2} \right)^{1/2} A^0, \quad (2)$$

where the one-body contribution to the axial charge A^0 is simply the nonrelativistic limit of the matrix element of $\gamma_5 \gamma_0$,

$$A^0 = -\frac{\sigma_1}{2M} \cdot (\mathbf{p}_1 + \mathbf{p}'_1) \tau_0^1 + 1 \leftrightarrow 2. \quad (3)$$

Here the two nucleons are labeled 1 and 2 and the initial (final) momentum of nucleon one is p_1 (p'_1).

The 3P_1 initial wave function (with z projection M) is

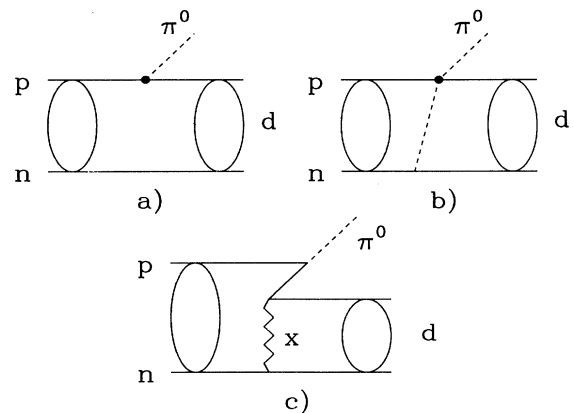


FIG. 1. Contribution to $NN \rightarrow d\pi$: one-body term (a), pion rescattering term (b), MEC contribution (c) for $x = \sigma$ or ω mesons.

$$|pn\rangle = -i(12\pi)^{1/2} \left[\frac{u_1^1(r)}{pr} \right] |^3P_1\rangle_M, \quad (4)$$

with u_1^1 the 3P_1 distorted wave which is normalized as $r \rightarrow \infty$,

$$u_1^1(r) \rightarrow \sin(pr - \pi/2 + \delta), \quad (5)$$

with p the initial relative momentum and δ the 3P_1 phase shift. The final deuteron wave function has s -wave (u) and d -wave (w) components,

$$|d\rangle = \frac{u(r)}{r} |^3S_1\rangle_M + \frac{w(r)}{r} |^3D_1\rangle_M, \quad (6)$$

normalized according to

$$\int_0^\infty dr [u(r)^2 + w(r)^2] = 1. \quad (7)$$

The spin angle functions in Eqs. (4) and (6) with Z projection M are

$$|^3L_J\rangle = \sum_{m_s, m_L} \langle 1m_s L m_L | JM \rangle Y_{L m_L} \chi_{m_s}^3. \quad (8)$$

The matrix element of A^0 with these wave functions is easily calculated [5]. The matrix element vanishes for $M = 0$ while the $M = 1$ or $M = -1$ result is

$$|\langle d|A^0|pn\rangle|^2 = \frac{16\pi}{M^2 m_\pi} |I_s^1 + \frac{1}{2^{1/2}} I_d^1|^2. \quad (9)$$

Here the dimensionless s -wave (I_s^1) and d -wave (I_d^1) integrals are defined as

$$I_s^1 = \frac{m_\pi^{1/2}}{p} \int_0^\infty dr u(r) \left(\frac{d}{dr} + \frac{1}{r} \right) u_1^1(r), \quad (10)$$

and

$$I_d^1 = \frac{m_\pi^{1/2}}{p} \int_0^\infty dr w(r) \left(\frac{d}{dr} - \frac{2}{r} \right) u_1^1(r). \quad (11)$$

The total cross section for $pn \rightarrow d\pi^0$ is easily calculated from this matrix element,

$$\sigma_{pn} = \left(\frac{f^2}{4\pi} \right) \frac{\eta}{2} (m_\pi M)^{1/2} |\langle d|A^0|pn\rangle|^2, \quad (12)$$

where η is the pion momentum in units of the pion mass m_π .

Our result for the cross section is then

$$\sigma_{pn} = \frac{f^2}{4\pi} \left[\frac{8\pi\eta}{M^{3/2} m_\pi^{1/2}} \right] \left| I_s + \frac{1}{2^{1/2}} I_d \right|^2, \quad (13)$$

where the total s -wave integral (I_s) has contributions from the one-body term, and, as we describe below, pion rescattering (I_s^π) and σ (I_s^σ) and ω (I_s^ω) MEC,

$$I_s = I_s^1 + I_s^\pi + I_s^\sigma + I_s^\omega. \quad (14)$$

Likewise, the total d -wave integral is,

$$I_d = I_d^1 + I_d^\pi + I_d^\sigma + I_d^\omega. \quad (15)$$

Pion rescattering was modeled in Ref. [5] with a phenomenological πN Hamiltonian which reproduces measured πN scattering lengths. The results of Ref. [5] are

$$I_s^\pi = I_s^2 + I_s^3, \quad (16)$$

$$I_s^2 = - \left(\lambda_1 + \frac{3}{2} \lambda_2 \right) \frac{m_\pi^{1/2}}{p} \int_0^\infty dr u(r) \left[\frac{f_\pi(r)}{m_\pi} \right] \left(\frac{d}{dr} + \frac{1}{r} \right) u_1^1(r), \quad (17)$$

$$I_s^3 = - \left(\lambda_1 + \frac{3}{2} \lambda_2 \right) \left(2 \frac{M}{m_\pi} + \frac{1}{2} \right) \frac{m_\pi^{1/2}}{p} \int_0^\infty dr u(r) u_1^1(r) \frac{d}{dr} \left[\frac{f_\pi(r)}{m_\pi} \right], \quad (18)$$

and

$$I_d^\pi = I_d^2 + I_d^3, \quad (19)$$

$$I_d^2 = - \left(\lambda_1 + \frac{3}{2} \lambda_2 \right) \frac{m_\pi^{1/2}}{p} \int_0^\infty dr w(r) \left[\frac{f_\pi(r)}{m_\pi} \right] \left(\frac{d}{dr} - \frac{2}{r} \right) u_1^1(r), \quad (20)$$

$$I_d^3 = - \left(\lambda_1 + \frac{3}{2} \lambda_2 \right) \left(2 \frac{M}{m_\pi} + \frac{1}{2} \right) \frac{m_\pi^{1/2}}{p} \int_0^\infty dr w(r) u_1^1(r) \frac{d}{dr} \left[\frac{f_\pi(r)}{m_\pi} \right]. \quad (21)$$

Here the pion propagator is

$$f_\pi(r) = \frac{1}{r} e^{-\mu r}, \quad (22)$$

where the effective mass $\mu = \sqrt{m_\pi^2 - l_0^2} = (\frac{3}{4})^{1/2} m_\pi$ for an energy transfer (in the center of mass frame at threshold) of $l_0 = m_\pi/2$.

The parameters λ_1 and λ_2 are related to the isospin 1/2 and 3/2 πN s -wave scattering lengths. We use values of [2,5,6],

$$\lambda_1 = 0, \quad \lambda_2 = 0.045. \quad (23)$$

Note, given the large λ_2 , any uncertainty in the small λ_1 is unimportant.

Unfortunately, this model of rescattering neglects form factors at the hadronic vertices. Instead, we adopt a slightly different philosophy. We simply evaluate, using perturbation theory, a few simple diagrams which we believe make the dominant contributions. Thus, we model the rescattering process as proceeding through the $\pi - \rho$ diagram of Fig. 2. If one considers the limit $m_\rho \rightarrow \infty$ and adjusts the $\pi - \rho$ coupling constant to reproduce the πN scattering lengths, then the diagram in Fig. 2 will reproduce Eqs. (16)–(22).

Figure 2 now provides a prescription for including form factors. There will be form factors at the two meson-nucleon vertices and the propagator for the ρ meson. The largest effect should be the ρ propagator (assuming the meson-nucleon form factors have shorter range). This modifies Eq. (22) to

$$f_\pi(r) = \frac{m_\rho^2}{m_\rho^2 - \mu^2} (e^{-\mu r} - e^{-m_\rho r})/r \quad (24)$$

without changing predictions for the πN scattering lengths. Thus, we evaluate rescattering as in Ref. [5]

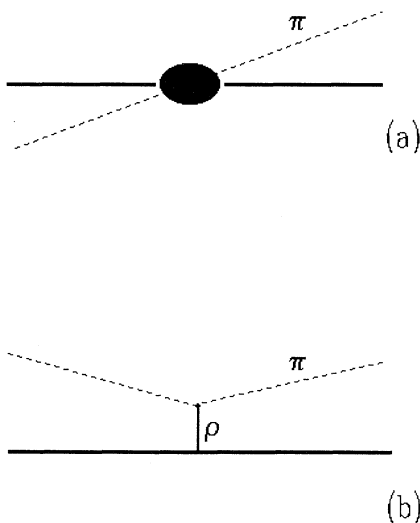


FIG. 2. Pion-nucleon s -wave scattering (a) modeled via ρ meson exchange (b) with the $\pi\pi\rho$ coupling adjusted to reproduce the s -wave πN scattering length. This represents the black dot in Fig. 1(b).

except that Eq. (22) is replaced by Eq. (24). This represents a minimal inclusion of a form factor and leads to a decrease in the cross section (see Sec. III) of about 20%. The inclusion of additional meson-nucleon form factors will presumably lead to further (although smaller) reductions. More detailed investigations of rescattering (including calculations in three-body models) would be very useful; see Sec. IV.

Finally we include heavy meson exchange as in Ref. [2]. The contribution of σ meson exchange in Fig. 1(c) gives

$$I_s^\sigma = \frac{m_\pi^{1/2}}{p} \int_0^\infty dr u(r) \left[\frac{f_\sigma(r)}{M} \right] \left(\frac{d}{dr} + \frac{1}{r} \right) u_1^1(r), \quad (25)$$

and

$$I_d^\sigma = \frac{m_\pi^{1/2}}{p} \int_0^\infty dr w(r) \left[\frac{f_\sigma(r)}{M} \right] \left(\frac{d}{dr} - \frac{2}{r} \right) u_1^1(r), \quad (26)$$

with (neglecting form factors for the moment),

$$f_\sigma(r) = \frac{g_\sigma^2}{4\pi r} e^{-m_\sigma r}. \quad (27)$$

The ω exchange contribution is

$$I_s^\omega = \frac{m_\pi^{1/2}}{p} \int_0^\infty dr u(r) \left[\frac{f_\omega(r)}{M} \right] \left(\frac{d}{dr} + \frac{1}{r} \right) u_1^1(r), \quad (28)$$

and

$$I_d^\omega = \frac{m_\pi^{1/2}}{p} \int_0^\infty dr w(r) \left[\frac{f_\omega(r)}{M} \right] \left(\frac{d}{dr} - \frac{2}{r} \right) u_1^1(r), \quad (29)$$

with

$$f_\omega(r) = \frac{g_\omega^2}{4\pi r} e^{-m_\omega r}. \quad (30)$$

Note, there is no term in Eq. (28) involving $d/dr f_\omega(r)$. This term was present in the $pp \rightarrow pp\pi^0$ calculations of Refs. [2,3] but is proportional to $\sigma_1 \times \sigma_2$ which has a vanishing matrix element here. We neglect the very small contributions of δ and ρ mesons in Fig. 1(c). These gave almost no contribution in Ref. [2]. The last step is to modify Eqs. (27) and (30) as in Eq. (A.28) of Ref. [7] to include meson-nucleon form factors.

The calculation is summarized as follows. The cross section is given by Eq. (13) with the s -wave (I_s) and d -wave (I_d) integrals having contributions from one-body, Eqs. (10), (11), pion rescattering, Eqs. (16)–(21), and heavy meson exchange, Eqs. (25)–(30). The parameters in the model are the pion nucleon coupling (where we use the recent value [8]),

$$\frac{f^2}{4\pi} = 0.075, \quad (31)$$

and the rescattering parameters λ_1 and λ_2 which are fit to reproduce πN scattering lengths [6] [and we use the values in Eq. (23)]. Finally the σ and ω meson coupling constants, masses and form factor cutoff parameters are taken (in general) from the one-boson-exchange potentials used to generate the 3P_1 (and deuteron) distorted

TABLE I. Contributions to the matrix element for $NN \rightarrow d\pi$ from one-body (I^1), pion rescattering (I^π), and $\sigma + \omega$ meson exchange currents (I^σ, I^ω) for various potential models, see Eqs. (14)–(30).

Model	I_s^1	$I_d^1/2^{1/2}$	I_s^π	$I_d^\pi/2^{1/2}$	I_s^σ	$I_d^\sigma/2^{1/2}$	I_s^ω	$I_d^\omega/2^{1/2}$
RSC [9]	0.081	-0.093	0.120	0.035	0.032	0.000	0.026	0.000
BPA(R) [7]	0.095	-0.081	0.119	0.026	0.039	0.000	0.032	0.000
Pairs [10]	0.086	-0.086	0.116	0.031	0.034	0.001	0.028	0.001

waves. There are no parameters fit to pion production data.

III. RESULTS

In this section we present results for the total cross section. Near threshold, the energy dependence of the $np \rightarrow d\pi^0$ total cross section is expected to be [4],

$$\sigma_{np} = \frac{1}{2}(\alpha\eta + \beta\eta^3), \quad (32)$$

where α and β are constants. Note, we compare to TRIUMF np data [4]. To compare to charged pion production data one must consider Coulomb effects on the pion. Simple isospin considerations give for the related reaction $pp \rightarrow d\pi^+$ [4],

$$\sigma_{pp} = \alpha C_0^2 \eta + \beta C_1^2 \eta^3, \quad (33)$$

where $C_i(\eta)$ accounts for the reduction in the cross section due to the Coulomb barrier between the deuteron and the charged pion. Since we only calculate s -wave pion production we only calculate the constant α . Furthermore, we have not calculated the Coulomb factor C_0 .

The experimental value for α is [4]

$$\alpha = 184 \pm 5 \pm 13 \mu\text{b}, \quad (34)$$

where the first error is statistical and the second includes a 5% systematic error in the spectrometer acceptance and a 5% scale uncertainty in the np elastic cross section (which was used for normalization). To calculate a theoretical α we simply evaluate the cross section, Eq. (13), at a single near threshold energy and divide by $\eta/2$.

We will present results for a variety of potential models including the Reid soft core (RSC) potential [9], Paris [10], and three slightly different Bonn r -space one-boson-exchange potentials: OBEPR [11] and models A and

TABLE II. Cross section factor α , Eqs. (32), (33), for different potential models both with and without σ and ω MEC. Note the same potential model is used for the initial 3P_1 and final deuteron wave function.

Model [reference]	α (with MEC)	α (without MEC)
	μb	μb
RSC [9]	175	88.5
Pairs [10]	192	94.1
BPA(R) [7]	230	110
BPB(R) [7]	203	103
OBEPR [11]	215	109
Average	203 ± 21	101 ± 9

B of Appendix A of [7] which we refer to as BPA(R) and BPB(R). In addition, we consider deuteron wave functions from a number of momentum-space potentials including the full energy-dependent Bonn model [11] (which we call BonnE) and the one-boson-exchange potentials BonnA(Q) [7], BonnB(Q) [7], and BonnC(Q) [7]. All of these models reproduce the 3P_1 phase shifts and the low energy deuteron parameters such as the binding energy. Together they represent a fairly broad range of deuteron d -state probabilities and short-distance wave functions.

Table I lists various contributions to the matrix element. There is important cancellation between the s - and d -wave one-body terms. The largest contribution is the pion rescattering. The σ and ω mesons make about equal contributions. This is different from $pp \rightarrow pp\pi^0$ where the σ meson provides the dominant MEC [2].

Table II lists values of α for five different potential models. Calculations with MECs give results from 175 to 230 μb in good agreement with experiment. Calculations without MECs range from 88.5 to 110 μb , about a factor of two smaller. The Reid soft core potential has the smallest wave function at short distances (for both the deuteron and 3P_1) and gives the smallest cross section.

Our results without MECs are consistent with the early Koltun and Reitan calculations [5] given two differences. Koltun and Reitan calculated an α from 146 to 160 μb (depending on the potential model used). However, they used an old (large) value for the pion coupling of $f^2/4\pi = 0.088$. Changing to the modern value, Eq. (31), will reduce their α by 15% to values ranging from 124 to 136 μb .

The remaining difference concerns form factors in the pion rescattering contribution. Koltun and Reitan ig-

TABLE III. Cross section factor α Eqs. (32), (33) for the RSC potential model [9] 3P_1 initial wave function and various deuteron wave functions.

Deuteron	α (with MEC)	α (without MEC)
	μb	μb
RSC	175	88.5
Pairs	204	97.7
BonnE	228	97.3
BonnA(Q)	272	121.2
BonnB(Q)	256	115
BonnC(Q)	243	110
OBEPR	245	114
BPA(R)	249	115
BPB(R)	231	108

TABLE IV. Same as Table III except for the Paris [10] 3P_1 initial wave function.

Deuteron	α (with MEC)	α (without MEC)
	μb	μb
RSC	170	86.3
Pairs	192	94.1
BonnE	204	90.4
BonnA(Q)	244	113
BonnB(Q)	232	108
BonnC(Q)	222	104
OBEPR	225	108
BPA(R)	227	108
BPB(R)	214	102

TABLE V. Same as Table III except for the Bonn r -space potential BPA(R) [7] 3P_1 initial wave function.

Deuteron	α (with MEC)	α (without MEC)
	μb	μb
RSC	168	86
Pairs	192	94.2
BonnE	209	91.6
BonnA(Q)	248	114
BonnB(Q)	235	108
BonnC(Q)	224	104
OBEPR	227	108
BPA(R)	230	110
BPB(R)	215	103

TABLE VI. Same as Table III except for the Bonn r -space potential BPB(R) [7] 3P_1 initial wave function.

Deuteron	α (with MEC)	α (without MEC)
	μb	μb
RSC	163	87.2
Pairs	183	94.7
BonnE	193	91.4
BonnA(Q)	231	113
BonnB(Q)	219	108
BonnC(Q)	210	104
OBEPR	213	108
BPA(R)	216	109
BPB(R)	203	103

TABLE VII. Same as Table III except for the Bonn r -space potential OBEPR [11] 3P_1 initial wave function.

Deuteron	α (with MEC)	α (without MEC)
	μb	μb
RSC	158	86
Pairs	181	94.3
BonnE	197	92.2
BonnA(Q)	235	115
BonnB(Q)	222	109
BonnC(Q)	212	105
OBEPR	215	109
BPA(R)	217	109
BPB(R)	203	103

nored all form factors. Instead we include the ρ meson propagator in Eq. (24). This reduces the cross section by another 20%. Alternatively, if we set $m_\rho = \infty$ in Eq. (24), in order to compare to Koltun and Reitan, then the rescattering integrals for the Reid soft core potential become $I_s^\pi = 0.132$ and $I_d^\pi = 0.038$ in place of those in Table I. The cross section factor α (without MECs) now ranges from 109 (Reid) to 133 (OPEPR) μb . This range is consistent with that of Koltun and Reitan (once f^2 is corrected).

To study how the results depend separately on the initial and final wave functions, we have calculated α for many different combinations of deuteron and 3P_1 wave functions. These results are presented in Tables III through VII. Note, MEC contributions for calculations with Reid soft core or Paris 3P_1 wave functions use coupling constants and form factors from BonnA(R). All other calculations use parameters from the potential used for the 3P_1 wave function. We expect results to be insensitive to the choice of MEC parameters.

Changes in the d -state percentage of the deuteron from 4.38% for BonnA(Q) to 4.99% for BonnB(Q) to 5.61% for BonnC(Q) only changes the cross section by about 10%. Instead changing from a model such as the Reid Soft Core potential (with a relatively repulsive core and a small short distance deuteron wave function) to a softer Bonn model (with a larger short distance wave function) leads to a 20% or more increase in the cross section.

Thus if the MEC current operator and the treatment of pion rescattering are under control, $NN \rightarrow d\pi$ can tell something about the short distance NN wave function (rather than the strength of the tensor force). However, much more work is needed on rescattering and MEC before this can be done quantitatively.

IV. SUMMARY AND CONCLUSIONS

We have calculated the total cross section for $pn \rightarrow d\pi^0$ and $pp \rightarrow d\pi^+$ very near threshold in a simple perturbative model. Contributions from one-body terms, pion rescattering, and σ and ω meson exchange currents (MEC) were included. We find that calculations with MEC are in good agreement with a recent TRIUMF measurement while calculations without MEC are almost a factor of two smaller. Thus the MEC mechanism proposed to explain a large enhancement in the $pp \rightarrow pp\pi^0$ cross section is fully consistent with the $NN \rightarrow d\pi$ data. This is interesting because the deuteron channel tests different spin and isospin matrix elements of the MEC compared to the pp final state.

Finally, the largest contribution to $NN \rightarrow d\pi$ is from pion rescattering. We only calculated this to lowest order. Further studies of pion rescattering in three-body models would be very useful.

ACKNOWLEDGMENTS

We thank Charlotte Elster for providing deuteron wave functions for the OBEPR, BPA(R), and BPB(R) potentials. Useful discussions with H. O. Meyer and S. Schramm are also noted. This work was supported in part by DOE Grant No. DE-FG02-87ER-40365.

- [1] H.O. Meyer, C.J. Horowitz, H. Nann, P.V. Pancella, S.F. Pate, R.E. Pollack, B. von Przewoski, T. Rinckel, M.A. Ross, and F. Sperisen, Nucl. Phys. **A539**, 633 (1992).
- [2] C.J. Horowitz, H.O. Meyer, and D.K. Griegel, Phys. Rev. C (submitted).
- [3] T.S.H. Lee and D.O. Riska, Phys. Rev. Lett. **70**, 2237 (1993).
- [4] D.A. Hutcheon *et al.*, Nucl. Phys. **A535**, 618 (1991).
- [5] D.S. Koltun and A. Reitan, Phys. Rev. **141**, 1413 (1966).
- [6] J. Spuller *et al.*, Phys. Lett. **67B**, 479 (1977); W. Beer *et al.*, Phys. Lett. B **261**, 16 (1991).
- [7] R. Machleidt, Adv. Nucl. Phys. **19**, 189 (1989).
- [8] J. R. Bergervoet *et al.*, Phys. Rev. C **41**, 1435 (1990); V. Stoks, R. Timmermans, and J.J. de Swart, Phys. Rev. C **47**, 512 (1993).
- [9] R.V. Reid, Ann. Phys. (N.Y.) **50**, 411 (1968).
- [10] M. Lacombe, B. Loiseav, J.M. Richard, R. Vinh Mau, J. Cote, P. Pires, and R. de Tourreil, Phys. Rev. C **21**, 861 (1980).
- [11] R. Machleidt, K. Holinde, and C. Elster, Phys. Rep. **149**, 1 (1987).